

IL NUOVO CIMENTO
DOI 10.1393/ncc/i2008-10324-3

VOL. 31 C, N. 5-6

Settembre-Dicembre 2008

Filtered deterministic waves and analysis of the fractal dimension of the components of the wind velocity

M. TIJERA⁽¹⁾(*), J. L. CANO⁽¹⁾(**), D. CANO⁽²⁾, D. BOLSTER⁽³⁾
and J. M. REDONDO⁽⁴⁾

⁽¹⁾ *Departamento de Física de la Tierra, Astronomía y Astrofísica (II)*
Universidad Complutense de Madrid - Madrid, Spain

⁽²⁾ *Agencia Estatal de Meteorología - Madrid, Spain*

⁽³⁾ *Department of Geotechnical Engineering and Geosciences, UPC - Barcelona, Spain*

⁽⁴⁾ *Departamento de Física Aplicada, Universitat Politècnica de Catalunya - Barcelona, Spain*

(ricevuto l' 1 Ottobre 2008; approvato il 20 Dicembre 2009; pubblicato online il 27 Marzo 2009)

Summary. — The difficulty in developing models for waves in turbulent flows is a key problem in the analysis of the complexity of turbulence. We present a method to find and filter perturbations that are generated by the flow of deterministic waves from the power spectrum in the atmospheric boundary layer (ABL). The perturbation model proposed assumes that the amplitude and frequency of such waves decay with time exponentially. For illustrative purposes, we apply the technique to three time series of wind velocities obtained with a sonic anemometer. This analytical procedure allows us to filter waves of the proposed structure with a 99% significance level in the power spectrum. We have applied the same method to 540 such wind series, all painting similar results. We then compare the fractal dimension of the original series to those from which the waves have been removed. We find that the fractal dimension of the filtered waves is slightly less than that of the original series. Finally, we consider the fractal dimension of the studied series as a function of the length-scales and dissipation rate of kinetic energy per unit mass. Our results suggest an increase of fractal dimension with both length-scale and dissipation rate of kinetic energy.

PACS 93.90.+y – Other topics in geophysical observations, instrumentation, and techniques.

1. – Introduction

Turbulence is one of the great unsolved problems of classical physics. Understanding the deterministic character of turbulent fluxes within the chaotic trajectory of turbulence plays an important role in its study. Often, methods based on power spectra of real turbulent data series are used to extract and study this deterministic component. Several studies have used power spectrum analysis in the study of climatic data series (*e.g.*, [1-3]) as well as turbulent wind data (*e.g.*, [4, 5]).

(*) E-mail: manueltijera@ono.com

(**) E-mail: jlcano@fis.ucm.es

In this work we propose a model and method based on power spectrum analysis to single out perturbations that arise in the mean wind flow due to the presence of deterministic waves. These waves can originate from the interaction of wind with topography (hills, trees, stones, etc.), by wind stress fluctuations as well as from other processes due to gradients of temperature and pressure that can exist at various points in the atmosphere. Although we cannot directly observe these waves with our experiments, we can track waves of a certain nature by means of the method we propose below using power spectrum data. We use the methods of Blackman and Tuckey [6] to calculate the power spectra. We also follow the methods of Crutchfield *et al.* [7] and Cvitanovic [8], who developed tools to analyse dynamic systems within turbulent flows. In this paper we focus on analysing deterministic waves that are immersed in atmospheric turbulent flows within the boundary layer. The technique to determine and filter deterministic waves from the power spectrum is applied to each of the components of velocity series measured with a sonic anemometer.

The method we propose is limited if there are irregularities within a power series or if there are peaks that are not well represented by our model. Nonetheless for the data presented here the method appears to work well.

After applying our proposed technique we use the results to calculate the Hausdorff-Besicovitch fractal dimension [9-11] of both the original series of wind velocities and those where we have filtered out the deterministic waves. We then compare the values in both dimensions. Next we study the behaviour of the fractal dimension with the characteristic length scales of the filtered waves and the energy of dissipation of these waves. We aim to gain some understanding of the relationship between the structure of a turbulent flow and its fractal dimension. It will allow us to understand if larger fractal dimension implies more dissipation. Other variables such as the energy of dissipation and length scales of the filtered waves cause changes in the structure of the flow. We aim to see if changes in the fractal dimension can be related with changes in these variables.

2. – Method to identify and filter deterministic waves

When the power spectrum of a time series of wind velocities is calculated maximum values can appear that are identified as peaks. In particular we consider peaks with a significance level greater than 99%. Such peaks typically occur due to periodic and deterministic structures in turbulent flows. We propose the following wave model to capture the shape of the peak appearing in the power spectrum:

$$(1) \quad y(t) = Ae^{-\alpha t} \cos(2\pi f_0 e^{-\beta t} t),$$

where A is amplitude of the wave, f_0 is the frequency, α is the damping coefficient of the amplitude and β is damping coefficient of the frequency. This particular choice of wave has two decay features. First, we hypothesise that the amplitude A of a wave decays exponentially in time due to dissipation as the atmosphere is generally a dissipative medium in contact with the Earth's surface. Additionally we hypothesise that the frequency of the wave also decays exponentially in time, although at a different rate. The physical justification for this is less obvious. It is related to the dispersive nature of the atmosphere which cause the length of these waves to change. It is also justified *a posteriori* by the fact that the Fourier transform of such a wave displays a peak very similar to those that appear in our experimental power spectra. Initially we apply this

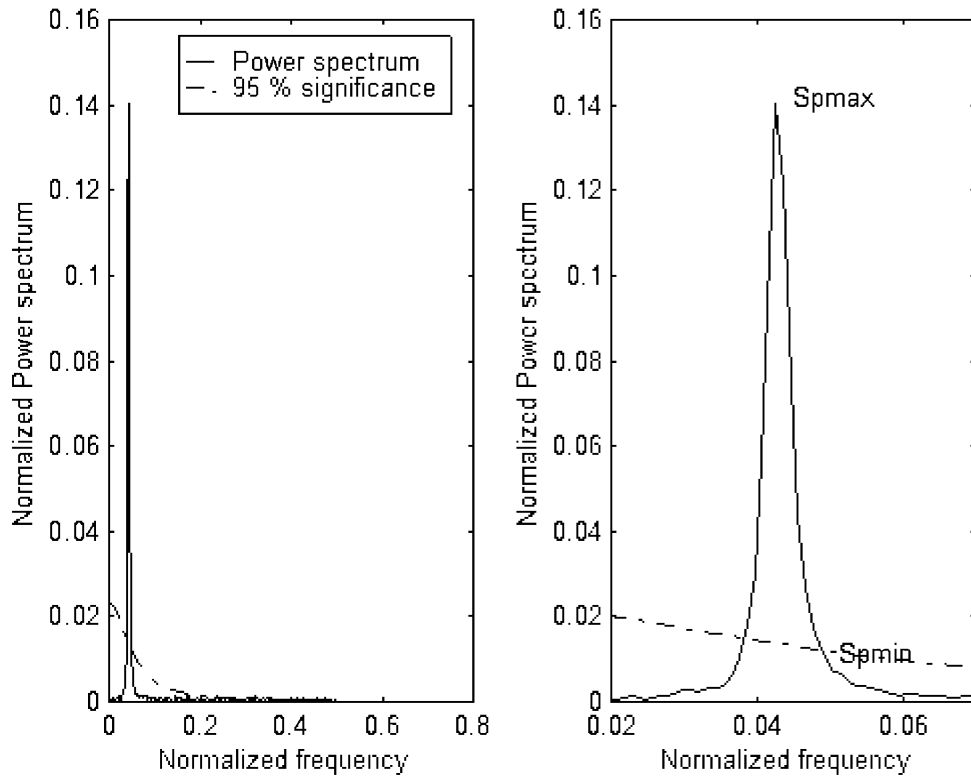


Fig. 1. – Power spectrum of random series plus a wave. We mark on the right graphic the maximum and minimum of the power spectrum that we take to deduce β .

method to synthetic data series that were generated via simulations with the artificial addition of such a wave to random data.

This type of a wave might correspond to perturbations created by the oscillation of an obstacle within the flow [12]. The range, scale and irregularity of such obstacles can give rise to a variety of waves of different amplitude and frequencies.

The variations of coefficients α and β obtained from real wind velocity series are smooth. These measured parameters typically lie within the ranges $0 < \alpha < 1$ and $0.0001 < \beta < 0.0125$. When given a power spectrum we identify and calculate α and β by first determining β by means of linear regression. It relates the frequencies of the minimum and maximum of the power spectrum ($f_{Sp\ min}$, $f_{Sp\ max}$) to the β parameter in the right semibandwidth $\delta = 8$ lag. (see, for example, fig. 1). We then calculate α with another linear regression.

We illustrate this by an example shown in fig. 1. We obtain β from the fit

$$(2) \quad f_{Sp\ min} - f_{Sp\ max} = 0.144 + 6.889\beta \quad (r^2 = 0.998),$$

where r is the correlation coefficient. Our statistical estimation is greater than 99% and so our confidence of accuracy is high.

We then calculate the parameter α by generating five new time series with a variation of α , for each β proposed in the last paragraph, in an interval between 0 and 1. For

each value of β , we have a new series that allows us to find a linear relation between the damping coefficient α of the amplitude and the β parameter. For α we obtain

$$(3) \quad \alpha = 9.925 \tilde{\alpha} + b,$$

where

$$(4) \quad b = -41.504 \beta - 0.228$$

and

$$(5) \quad Sp_{\text{half}} = \frac{Sp_{\text{max}} \tilde{\alpha}^2}{(f_{Sp_{\text{half}}} - f_{Sp_{\text{max}}})^2 + \tilde{\alpha}^2}.$$

$\tilde{\alpha}$ is a constant of proportionality, Sp_{half} is the closest value to the half value of the maximum in the bandwidth 2δ and Sp_{max} is the maximum value of the power spectrum.

$f_{Sp_{\text{half}}}$ is the frequency where the power spectrum is closest value to Sp_{half} .

Once we have calculated these parameters, we calculate the amplitude of the wave. To do this we use a further hypothesis that the square of the amplitude of the wave is proportional to the difference of maximum and minimum power spectrum. This assumes that the total kinetic energy is equal to the sum of the kinetic energies of periodic perturbations and other causes that do not obey the proposed wave model, as for instance, the stochastic character of the wind series. Thus the wave amplitude is approximately given by

$$(6) \quad A \approx \sqrt{(Sp_{\text{max}} - Sp_{Ec \text{ min}})},$$

where Sp_{max} is the maximum non-normalized power spectrum, and $Sp_{Ec \text{ min}}$ is the non-normalized value of power spectrum that corresponds to the minimum of kinetic energy of the wave around bandwidth f_0 . The kinetic energy due to such effects ($Sp_{Ec \text{ min}}$) is removed from the maximum value of power spectrum at f_0 (Sp_{max}), so that we obtain the energy associated with the periodic perturbations.

This method has been applied to a real series of wind speeds for each of its components. It provides a simple manner to filter deterministic waves as the form (1). After this filtering we obtain a more stochastic series. The process of filtering allows us to study the stochastic nature of isotropic turbulence and features thereof, such as the Hausdorff-Besicovitch fractal dimension. We note that this dimension has been studied extensively in the literature (*e.g.*, [10,13-15]). There are several other studies that analyse wind velocities series with other methods to obtain the fractal dimension as correlation dimension of a strange attractor of atmospheric turbulence (*e.g.*, [16-21]).

3. – Applying method to real series of velocity wind

We applied the method described in the previous section to more than 540 wind velocity series. The anemometer used to acquire these data had a sample rate of 21 Hz, and the total time length of these series was 9.52 minutes (12000 data points) or 10 minutes (12600 data points). The data for this study was gathered in the area near the Almaraz Nuclear Power Plant (Cáceres, Spain), which is an open plateau region with no significant elevations in its vicinity. The analysis is performed on data sets which are

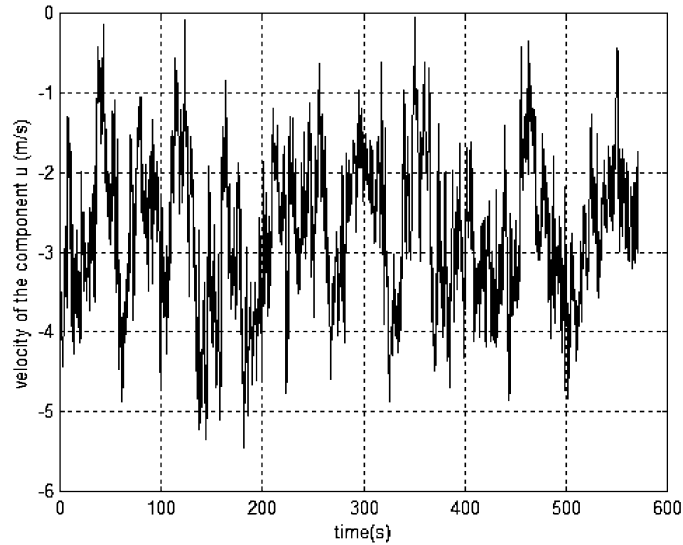


Fig. 2. – A time series for the velocity component along the direction $x(u0722)$.

smoothed at high frequencies so as to have a cleaner data set while maintaining the wave peaks we aim to capture.

Here we describe three examples, referring to each one of the three components x , y and z of the wind velocity from specific data sets. These data sets were chosen for illustrative purposes as they are representative of the general behaviour observed. We start by applying the suggested methodology to the wind velocity series named $u0722$. A plot of the data is shown in fig. 2. As the temporal variation for the three series that we analyse in this work show similar general behaviour we only plot this one for illustrative purpose.

The procedure we follow in order to filter any deterministic waves is

- 1) Calculate the power spectrum.
- 2) Look at the peaks of energy in the power spectrum with a value higher than the 99% significance level.
- 3) Once identified, we filter these peaks using the suggested methodology by subtracting (1) from the time series.
- 4) Evaluate the new power spectrum from the filtered series and reiterate the procedure until all such structures are removed.

The wave parameters that are filtered via this method for the three data series are indicated in table I. From this we note that the first waves being filtered are waves with larger amplitudes at lower frequencies. Progressively waves at higher frequencies with smaller amplitudes and lesser energies are filtered. In the first column we have the name of the series being considered. After filtering, we rename it as follows: the name of the original series with the lag number in which the deterministic wave is filtered. The lag number is a regular interval between two consecutive values in the power spectrum. In

TABLE I. – The parameters of all filtered waves are shown in the series that have been analysed in this paper: (a) u0722, (b) v1825, (c) w2328. Being f the normalized frequency, f_0 the real frequency, β the damping coefficient of the frequency, α the damping coefficient of the amplitude, A the amplitude of wave, \bar{u} is the mean wind velocity, λ the wavelength. In the seventh column the equation of the filtered wave is shown at frequency f_0 .

| a) | | | | | | | | |
|----------|-------|---------------|-------------------------------|--------------------------------|-----------------------------|--|-----------------------------------|---------------|
| Series | f | f_0 (Hz) | β (s ⁻¹) | α (s ⁻¹) | A (m s ⁻¹) | Equation of the filtered waves | \bar{u} (m s ⁻¹) | λ (m) |
| u07223 | 0.003 | 0.021 | 0.000295 | 0.265 | 12.18 | $y = 12.18e^{-0.265t} \cos(2\pi f_0 e^{-0.000295t} t)$ | 3.28 | 157.19 |
| u0722136 | 0.136 | 0.952 | 0.000295 | 0.371 | 0.7 | $y = 0.70e^{-0.371t} \cos(2\pi f_0 e^{-0.000295t} t)$ | 3.28 | 3.45 |

| b) | | | | | | | | |
|----------|-------|---------------|-------------------------------|--------------------------------|-----------------------------|---|-----------------------------------|---------------|
| Series | f | f_0 (Hz) | β (s ⁻¹) | α (s ⁻¹) | A (m s ⁻¹) | Equation of the filtered waves | \bar{u} (m s ⁻¹) | λ (m) |
| v182512 | 0.011 | 0.08 | 0.000304 | 0.567 | 5.84 | $y = 5.84e^{-0.567t} \cos(2\pi f_0 e^{-0.000304t} t)$ | 1.78 | 22.25 |
| v1825200 | 0.195 | 1.37 | 0.000365 | 0.152 | 0.63 | $y = 0.63e^{-0.152t} \cos(2\pi f_0 e^{-0.000365t} t)$ | 1.78 | 1.30 |

| c) | | | | | | | | |
|--------|--------|---------------|-------------------------------|--------------------------------|-----------------------------|---|-----------------------------------|---------------|
| Series | f | f_0 (Hz) | β (s ⁻¹) | α (s ⁻¹) | A (m s ⁻¹) | Equation of the filtered waves | \bar{u} (m s ⁻¹) | λ (m) |
| w23288 | 0.0076 | 0.053 | 0.00344 | 0.556 | 4.10 | $y = 4.10e^{-0.556t} \cos(2\pi f_0 e^{-0.000344t} t)$ | 1.11 | 20.80 |

the second column we have the normalized frequency f at which the wave is filtered. In the third column the real frequency f_0 . The fourth, fifth and sixth columns correspond, respectively, to the wave parameters, β the damping coefficient of the frequency, α the damping coefficient of the amplitude and A the amplitude of the wave. The seventh column indicates the governing equation of the filtered wave and in the last two columns the mean wind velocity \bar{u} of the series is indicated as well as the wavelength λ .

Figure 3 shows a zoom in of the power spectrum of the original series and of the series once the highest amplitude wave is filtered. An analysis of fig. 3 shows that the filtering procedure is effective, such that the power spectrum of the analysed maximum above the 99% significance level falls below this level once the filtering is performed. Some residual values can persist to exist between 95% and 99% significance levels, which are probably due to other effects not considered in the proposed model.

4. – Fractal dimension

In this section we calculate the Hausdorff-Besicovitch fractal dimension in the physical two-dimensional space (velocity-velocity) of the original series and the series from which the waves have been filtered. The velocity-velocity space in some sense represents correlations between different components of velocities. The flows presented here are turbulent, non-periodic and contain deterministic components. We calculate the fractal dimension to analyse the irregularity of these flows as the larger the fractal dimension, the more random the system. Thereby we hope to find a relationship between the fractal dimension and the deterministic nature of the flow. We approximate the Hausdorff-Besicovitch

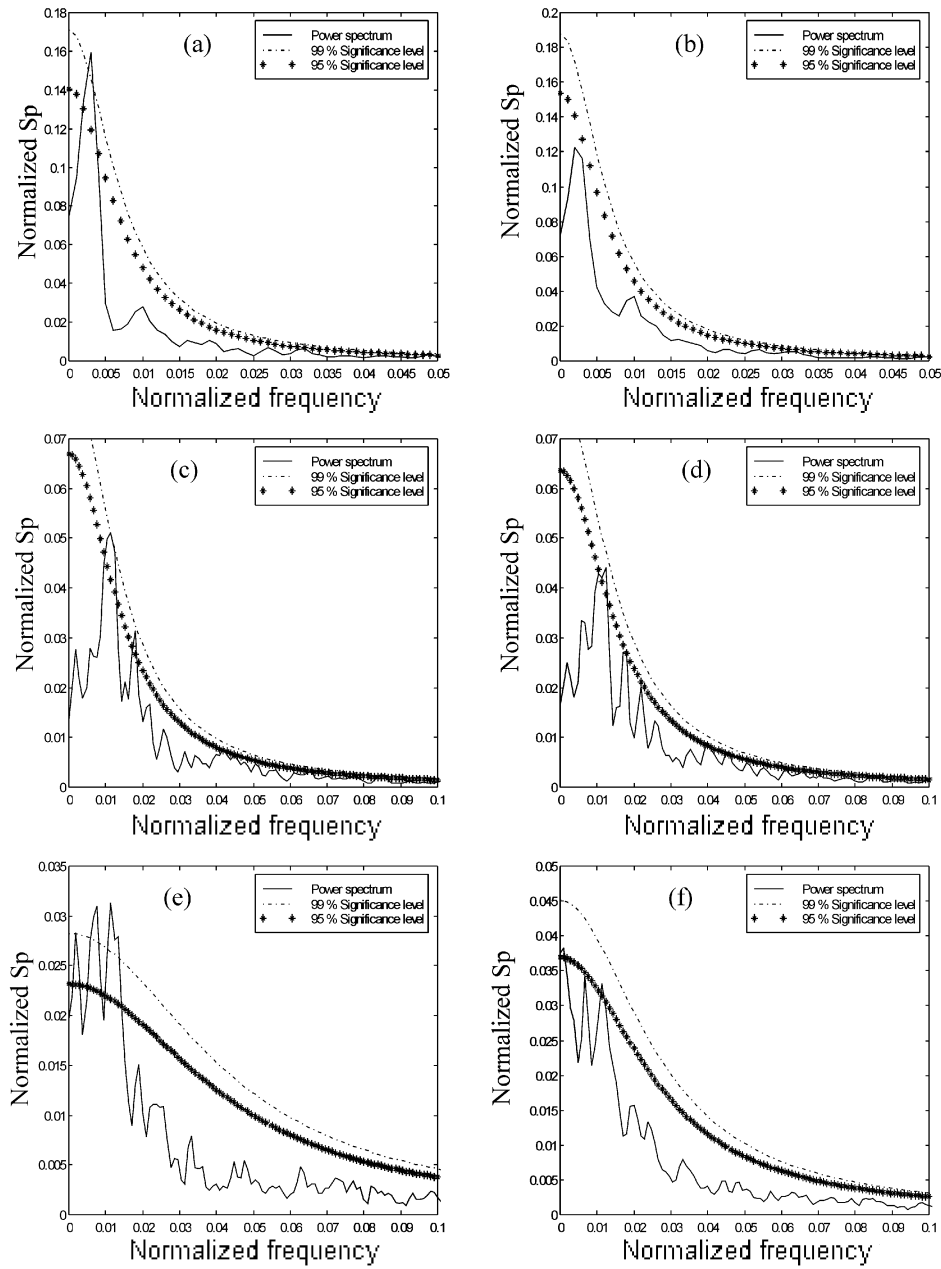


Fig. 3. – Zoom of the power spectrum of the original series ((a) $u0722$, (c) $v1825$ and (e) $w2328$) and series once filtered the first deterministic wave ((b) $u07223$, (d) $v182512$, and (f) $w23288$).

TABLE II. – *The values of the Hausdorff-Besicovitch dimension in the physical spaces (u - v) for the original series (first and second row) of the u and v components of the wind velocity of considered examples. The names of the series have been mentioned in the first column. In the second column the linear regression equations are indicated, in the third column the coefficient of correlation of these equations is showed and in the fourth column the values of the Hausdorff-Besicovitch dimension are indicated.*

| Series u and v | Regression equation | Coefficient of correlation | Hausdorff-Besicovitch dimension |
|---------------------|-----------------------|----------------------------|---------------------------------|
| $u0722$ y $v0722$ | $y = -1.422x + 1.533$ | $r = 0.996$ | 1.422 ± 0.027 |
| $u1825$ y $v1825$ | $y = -1.349x + 1.239$ | $r = 0.986$ | 1.349 ± 0.047 |

dimension by

$$(7) \quad d = \lim_{L \rightarrow 0} \frac{\log N(L)}{\log \left(\frac{1}{L}\right)}$$

which is known by many [22, 23] as the Kolmogorov capacity (box-counting dimension). $N(L)$ is the minimum number of boxes of side L to cover the set with the data in physical space (velocity-velocity). As L becomes smaller, N meets the following relation:

$$(8) \quad N(L) \cong kL^{-d},$$

where k is a constant. One motivation for calculating the Hausdorff-Besicovitch fractal dimension in physical space is that it provides a manner to locate a point in physical space with an accuracy of order L .

We use an algorithm that calculates the number of boxes of side L necessary to cover the different points that have been registered. By incrementally decreasing L we observe whether or not we approach the limit of eq. (7). Taking the logarithm of eq. (8) we obtain

$$(9) \quad \log N(L) = \log k - d \log L.$$

Then, by means of least-squares fitting between to data of $\log N(L)$ vs. $\log L$, for each one of the values of L considered, we obtain an equation for the straight line given by eq. (9). The fractal dimension is then given by the asymptotic slope d from eq. (9). For more details, we refer the interested reader to Russell *et al.* [24] and Sánchez [25]. To calculate $N(L)$ the space is divided into squares of side L . We apply the highest possible number of squares of various sizes, so that the result of the fractal dimension converges to values with small errors and high confidence.

For illustrative purposes, we consider two wind series from our complete data set and calculate their fractal dimension. We also calculate the fractal dimension of the same two series after we have filtered the deterministic waves described in sect. 2.

Figure 4 shows the relationship between $N(L)$ and L in a log-log plot. The slope of the straight line determined by the least-squares fitting gives us the fractal dimension of the u and v components of these series.

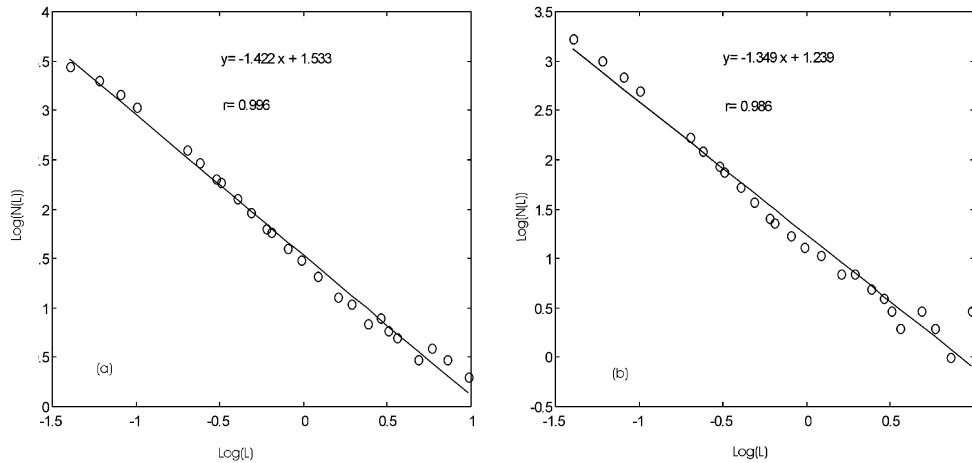


Fig. 4. – Linear regression between $\log N(L)$ and $\log L$. In the graph 25 points are plotted and each one of them corresponds to 25 squares of size L . Length L of the squares is indicated in table II. (a) $u0722$ and $v0722$, (b) $u1825$ and $v1825$.

The slopes of the straight line in fig. 4 (a) and (b) are obtained by the least-squares fitting and the slope and the y intercept constant for each equation are shown in table II. In all cases our r values and confidence levels are high. The fractal dimension is then the absolute value of the slope.

After removing the deterministic waves, using the methodology of sect. 2 we recalculate the fractal dimension in the same manner. The fractal dimension of the physical space (u, v) once filtered diminishes by approximately 7%. For the second series it diminishes by approximately 14%, suggesting that the presence of the waves increases the fractal dimension of the system.

In the same manner, for these same series we calculated the dimension for the physical spaces (u, w) and (v, w) . After filtering the fractal dimension diminishes by between 9-10%. The decrease of the fractal dimension of the series after filtering appears systematically in most of the 540 series that have been studied. The values of these dimensions, as was expected, are non-integer and always larger than 1 due to the dissipative nature of the atmosphere.

5. – Fractal dimension vs. length scales

In this section we analyse how the fractal dimension of each one of the three components of wind velocity varies with the length scales of the filtered waves in the physical space (velocity-time). For this work we analyse all 540 wind series. The length scale typically represents the characteristic size of the objects which generate the deterministic waves. It is given by $l \approx \bar{u}T$, where l is the length scale (that corresponds to the wavelength λ of table I), \bar{u} is the modulus of the mean wind speed and T is the period, that is equal to the reciprocal of the frequency at which the deterministic wave is filtered. We analyse each of the u, v and w components of the wind velocity.

In fig. 5 we plot the fractal dimension of wind velocity as defined in sect. 4 against the logarithm of the length scale. While, particularly at small scales there is a large

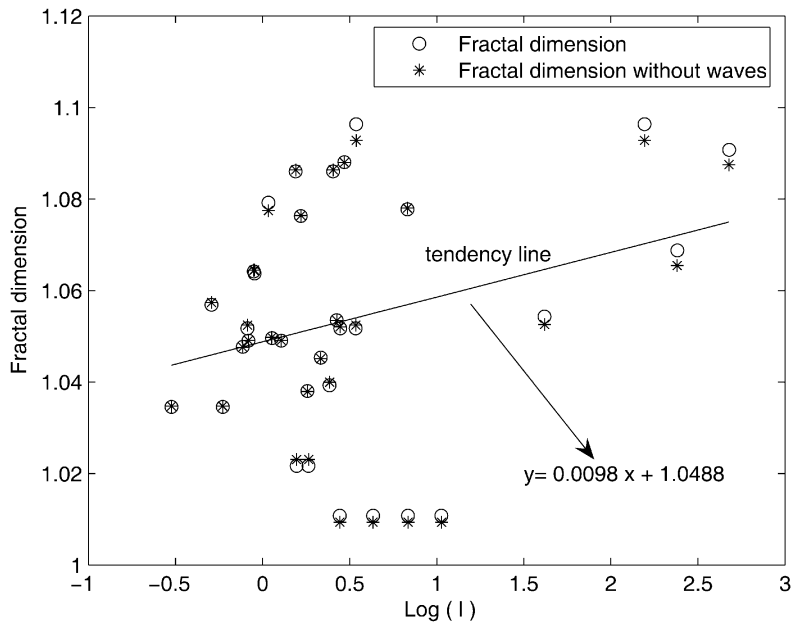


Fig. 5. – The variation of the fractal dimension *vs.* the logarithm length scales of the filtered waves of the *u* component of the wind velocity.

fluctuation in fractal dimension, there appears to be an increasing tendency in fractal dimension with increase in length scales, particularly for cases where $l > 10$ m. For length scales below 10 m, there is an oscillation around the mean fractal dimension of *u* component with no obvious trend (although there is a small rising trend).

In the same manner fig. 6 plots the fractal dimension for the *v* velocities against length scale. Here the increasing tendency is more obvious than for the *u* velocity. At smaller scales, where there appears to be some increasing trend, again this effect is less obvious at large scales.

The data for the vertical *w* velocity fields is shown in fig. 7. Here there appears to be no real dependence of fractal dimension on length scale. There is only an oscillation of the fractal dimension around the mean and little trend. This suggests that horizontal velocities are more significantly affected by the length scales.

6. – Variation of the fractal dimension *vs.* the dissipation energy

Finally, motivated by the observations of the previous section, we look into a relationship between the dissipation rate of kinetic energy per unit mass and the fractal dimension of the series for each of the components of the wind velocity. We estimate the rate of kinetic energy dissipation per unit mass of each of the filtered waves using Taylor's expression [26]

$$(10) \quad \langle \varepsilon \rangle \approx \frac{u^3}{l}.$$

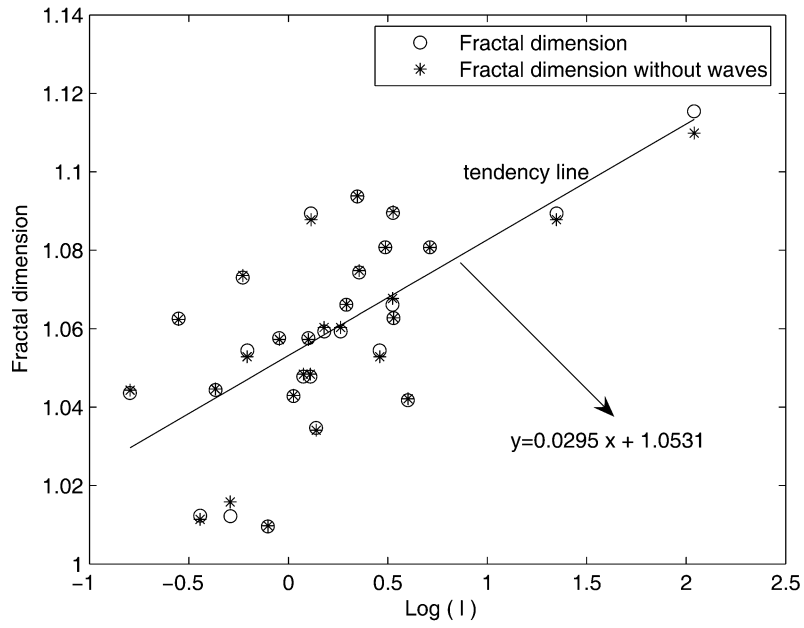


Fig. 6. – The variation of the fractal dimension *vs.* the logarithm length scales of the filtered waves of the *v* component of the wind velocity.

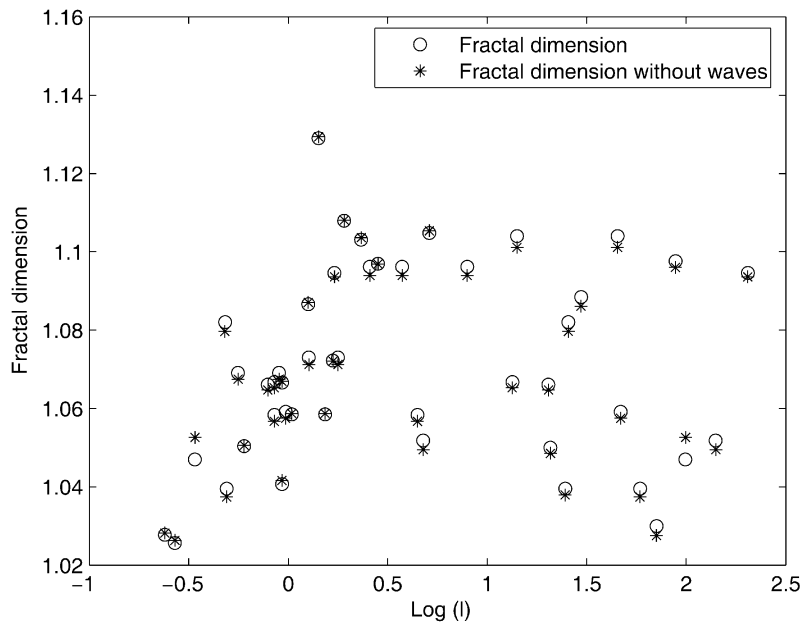


Fig. 7. – The variation of the fractal dimension *vs.* the logarithm length scales of the filtered waves of the *w* component of the wind velocity.

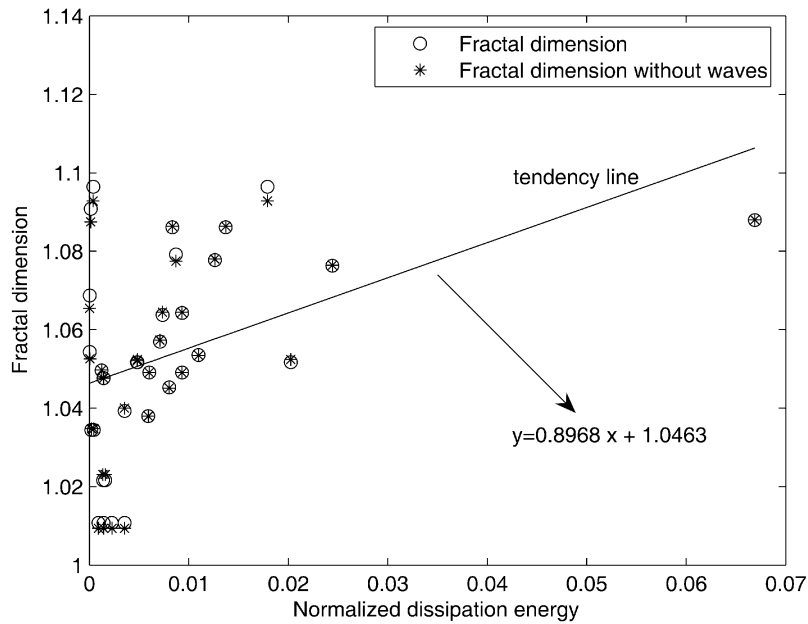


Fig. 8. – The variation of the fractal dimension *vs.* the normalized dissipation rate of kinetic energy per unit mass of the filtered waves of the *u* component of wind velocity.

The parameters *u* and *l*, described earlier, are both average statistical quantities. Figures 8, 9 and 10 show the variations of the fractal dimension *vs.* the dissipation rate of kinetic energy per unit mass of the *u*, *v* and *w* components, respectively.

From the data in fig. 8, we note a tendency for the fractal dimension to increase as the dissipation rate of kinetic energy per unit mass of the waves increases. To explain this trend we note that there is evidence that higher fractal dimension and higher dissipation rates go hand in hand. As such, the fractal dimension can be a parameter that gives some sort of measure of the rate of the dissipation within a turbulent flow. The deterministic waves that we filtered correspond to waves of the wind velocity. They cause the dissipation of large amounts of energy, because the atmosphere is a very dissipative system in contact with the terrestrial surface. The fact that the fractal dimension increases slightly with the release of higher amounts of energy makes us believe that an increase in the fractal dimension yields information on the growth of the stochastic character of the turbulence.

For the other horizontal velocity component, fig. 9 also illustrates an increase of fractal dimension with an increase in the energy of dissipation of the filtered waves.

Similarly there is an increasing trend in fig. 10 for the vertical velocities. Initially, this is slightly surprising, given that we found no increasing trend between length scale and fractal dimension of the vertical velocity in the previous section. From eq. (10) this leads us to believe that perhaps the influence of the u^3 terms dominates the length scale *l*.

7. – Conclusions

In this work we present a method to filter deterministic waves above the 99% significance level in power spectrum. After testing this method on synthetic data sets created

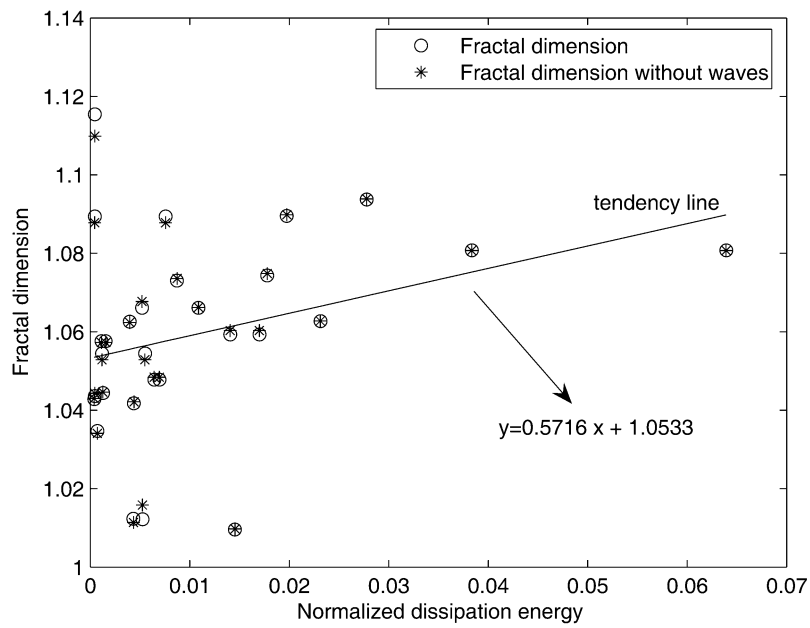


Fig. 9. – This graph shows the variation of the fractal dimension *vs.* the normalized dissipation rate of kinetic energy per unit mass of the filtered waves of the *v* component of wind velocity.

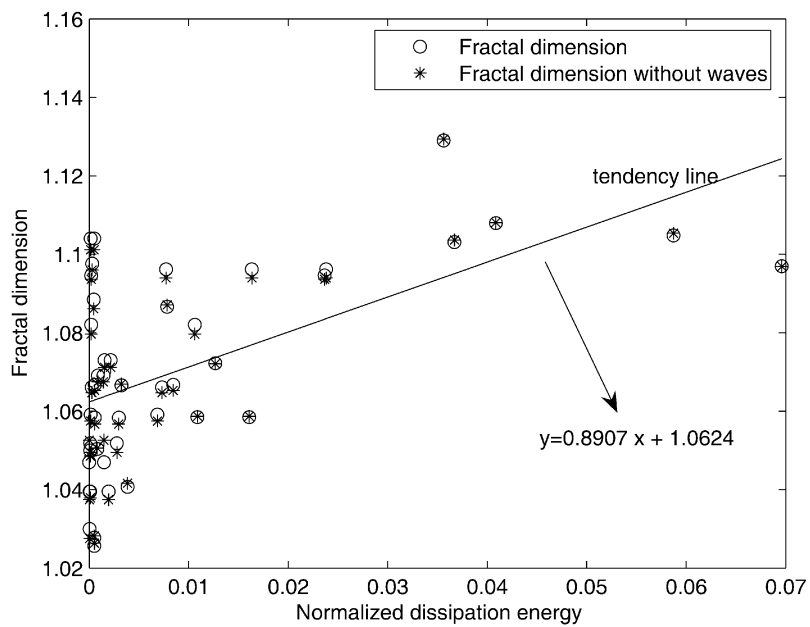


Fig. 10. – This graph shows the variation of the fractal dimension *vs.* the normalized dissipation rate of kinetic energy per unit mass of the filtered waves of the *w* component of wind velocity.

by simulation, we applied the method to a large set of wind data from a field site in Spain. We then compare fractal dimension of the raw data to that of the data after our proposed filtering method is conducted. Finally we look at the relationship between the length scales of the filtered deterministic waves and the fractal dimension of the flow velocities as well as the relationship between fractal dimension and kinetic energy dissipation. The results of our analyses led to three main conclusions:

- i) The fractal dimension of the series once filtered decreases roughly by 10% (7–14%) with respect to the original series. This appears in a systematic manner across most of the 540 series that have been studied.
- ii) There is an increasing tendency of the fractal dimension *vs.* higher length scales of the filtered waves for horizontal velocities at large length scales. For vertical velocities we observe merely an oscillation around the mean fractal dimension.
- iii) We find that the fractal dimension increases as the dissipation rate of kinetic energy per unit mass of the filtered waves increases.

* * *

We would like to thank Prof. Dr. C. YAGÜE for the advising in sample preparation and helpful discussions.

REFERENCES

- [1] NICOLIS C. and NICOLIS G., *Proc. Natl. Acad. Sci.*, **83** (1986) 536.
- [2] YIOU P., BAERT E. and LOUTRE M. F., *Surveys Geophys.*, **17** (1996) 619.
- [3] GHIL M., ALLEN M. R., DETTINGER M. D. *et al.*, *Rev. Geophys.*, **40** (2002) 1.
- [4] ARTIÑANO B., *Caracterización turbulenta de la capa superficial atmosférica en un terreno no homogéneo*, Thesis (Universidad Complutense de Madrid) 1988.
- [5] MAQUEDA BURGOS G., *Análisis y evolución de los parámetros turbulentos en la capa límite superficial atmosférica en base a datos de una torre meteorológica*, Thesis, Universidad Complutense de Madrid (1987).
- [6] BLACKMAN R. G. and TUCKEY J. W., *Measurement of power spectra from the point of view of Communication Engineering* (Dover, Mineola, New York) 1958.
- [7] CRUTCHFIELD J., FARMER D., PACKARD N., SHAW R., JONES G. and DONNELLY R. J., *Phys. Lett. A*, **76** (1980) 1.
- [8] CVITANOVIC PREDRAG, *Universality in Chaos* (Adam Hilger Ltd, Bristol) 1986.
- [9] HAUSDORFF F., *Math. Ann.*, **79** (1919) 157.
- [10] MANDELBROT B. B., *Fractal: Form, Chance, and Dimension* (Freemans, San Francisco) 1977.
- [11] FRAEDRICH K., *J. Atmos. Sci.*, **43** (1985) 419.
- [12] BOYER D. L. and DAVIES P. A., *Annu. Rev. Fluid Mech.*, **32** (2000) 165.
- [13] FEDER J., *Fractals* (Plenum, New York) 1988.
- [14] ADDISON P. S., *Fractals and Chaos* (Institute of Publishing Bristol and Philadelphia) 1997.
- [15] KORSH H. J and JODL H. J., *Chaos* (Springer-Verlag Berlin Heilderberg, New York) 1999.
- [16] HENDERSON H. W. and WELLS R., *Adv. Geophys.*, **30** (1988) 205.
- [17] TSONIS A and ELSNER J. E., *Nature*, **333** (1988) 545.
- [18] POVEDA-JARAMILLO G. and PUENTE C., *Boundary-Layer Meteorol.*, **64** (1993) 175.
- [19] SHIRER H. N., FOSMIRE C. J., WELLS R. and SUCIU L., *J. Atmos. Sci.*, **54** (1997) 211.
- [20] PALMER A. J., FAIRALL C. W. and KROPFLI R. A., *Nonlinear Proc. Geophys.*, **5** (1998) 13.

- [21] GALLEGO M. C., GARCIA J. A. and CANCELLO M. L., *Boundary-Layer Meteorol.*, **100** (2001) 375.
- [22] RUELLE D., *Chaotic Evolution and Strange Attractors* (Cambridge University Press, Cambridge) 1987.
- [23] VASSILICOS J. C. and HUNT J. C. R., *Proc. R. Soc. London, Ser. A*, **435** (1991) 505.
- [24] RUSSELL D. A., HANSON J. D. and OTT E., *Phys. Rev. Lett.*, **45** (1980) 1175.
- [25] SÁNCHEZ A., *Rev. Esp. Fís.*, **6** (1992) 22.
- [26] TAYLOR G. I., *Proc. R. Soc. London, Ser. A*, **151** (1935) 421.